An infrared absorption band caused by H^+ implantation in $LiNbO_3$ crystals

1991 J. Phys.: Condens. Matter 3 4145

(http://iopscience.iop.org/0953-8984/3/23/003)

J. Phys.: Condens. Matter 3 (1991) 4145–4150. Printed in the UK

An infrared absorption band caused by H^+ implantation in $LiNbO_3$ crystals

Xi-qi Feng†§, Tian-hao Shao‡§ and Ji-zhou Zhang†§

† Shanghai Institute of Ceramics, Academia Sinica, 1295 Dingxi Road, Shanghai 200050, People's Republic of China

‡ Shanghai Institute of Metallurgy, Academia Sinica, 865 Changning Road, Shanghai 200050, People's Republic of China

Received 14 August 1990, in final form 7 February 1991

Abstract. A new infrared absorption band at a wavenumber of about 3545 cm^{-1} has been observed in $LiNbO_3$ crystals implanted with energetic H^+ ions. It is found that the peak wavenumber of this band seems to be independent of the stoichiometry, dopant species and doping level in the investigated samples. The band, polarized perpendicular to the *c* axis, disappears after the sample was annealed in air at 500 °C for 0.5 h. The new absorption band is interpreted as a distributed *OH stretching vibration in a H^+-implanted* $LiNbO_3$. The displacement of Nb^{5+} ions from their regular sites (which was caused by the ion implantation) may expand the oxygen triangle to result in a longer O—O bond; this can explain the higher wavenumber of the OH band in the H^+-implanted $LiNbO_3$.

1. Introduction

$LiNbO_3$ crystals are of great importance for the formation of integrated optical elements and surface acoustic-wave devices. Helium or proton implantation has been used to modify the refractive index in defined regions to produce optical waveguides in the surface layer of $LiNbO_3$ [1–3]. Our earlier studies showed that heavy-ion (e.g. Xe^+, Ar^+ and N^+) implantation, caused stoichiometric decomposition in the near-surface of implanted $LiNbO_3$ but that H^+ implantation did not cause such decomposition [4]. However some near-surface properties of $LiNbO_3$ are affected by H^+ implantation. The appearance of a broad optical absorption band in the visible part of the spectrum and an increase in the relative dark conductivity in the surface layer have been observed experimentally [5]. These suggest that additional optical and electrically active centres are created after H^+ implantation. In some cases, certain reactions occur between the implanted H^+ and non-metal ions in the insulating material, resulting in the formation of a large concentration of XH groups (X≡O, C, F, etc) in the implanted region. The sharp line feature of the stretching vibration of the X—H bonds may be used in the defect identification. One example occurs in the vibrational modes of C—H and C—D bonds in SiC crystals implanted with H^+ and D^+ ions and used to locate the sites of the impurity atoms [6].

§ Also at: CCAST World Laboratory, PO Box 870, Beijing 100080, People's Republic of China.

0953-8984/91/234145 + 06 $03.50

Table 1. $LiNbO_3$ crystals used in the present study.

Sample	Li/Nb (in melt)	MgO in melt (mol%)	Cr_2O_3 in melt (mol%)	Fe_2O_3 in crystal (ppm)
1	0.945	0	—	—
2	1.01	0	—	—
3	0.945	5.0	—	—
4	0.945	6.0	—	—
5	0.945	6.0	—	530
6	0.945	0	0.1	—

The behaviour of hydrogen impurities in $LiNbO_3$ crystals is particularly conspicuous and it has been the subject of many recent investigations. Hydrogen is present in most as-grown $LiNbO_3$ crystals. When hydrogen is incorporated into $LiNbO_3$, an infrared absorption band can be observed; it is caused by the stretching vibration of OH dipoles. It was found that the peak-position, bandwidth and polarization dependence of the OH band can be affected by the change in the lattice environment resulting from the dopant or a change in crystal composition. Therefore the OH absorption band is an adequate tool for studying the interaction of hydrogen with neighbouring atoms in $LiNbO_3$, but so far little attention has been paid to the influence of H^+ implantation on the infrared absorption spectra of $LiNbO_3$. Recently, a new OH absorption band has been observed at about 3545 cm^{-1} in H^+-implanted $LiNbO_3$. It seems to be independent of the stoichiometry and dopants. In this paper, we describe the observed band and try to give an interpretation of the appearance of the new OH band.

2. Experiment

The $LiNbO_3$ crystals were pulled along the *c* axis using the Czochralski technique. After the growth process and annealing in air, the crystals were poled. The compositions of the various $LiNbO_3$ crystals used in the present study are listed in table 1. The crystals were cut parallel to the *c* axis and polished. Every crystal plate was cut into two samples. One was used for H^+ implantation and the other was used for comparison. The implanted samples are rectangularly shaped slabs, about 10 mm × 10 mm × 1 mm in size. Typical parameters for H^+ implantation are an ion energy of 50–200 keV, a dose of 3×10^{16} cm^{-2} and an implantation temperature of about 300 K. The infrared absorption spectra of OH vibrations and its polarization dependence were obtained using a Nicolet 7000 Fourier infrared spectrometer with a resolution better than 4 cm^{-1}. The unimplanted sample, which was obtained from the same crystal plate as the implanted sample, was used as a reference for the optical absorption measurement. The RBS–channelling technique was utilized to analyse radiation damage in $LiNbO_3$ induced by implantation. Because $LiNbO_3$ is an insulator, the sample surface was deposited with a layer of gold less than 30 Å thick before RBS measurement, in order to minimize the charge accumulation on the sample surface.

3. Experimental results

Ion implantation produces radiation damage and defects in $LiNbO_3$ crystals. Protons cause the least number of defects relative to other ions because hydrogen is the lightest

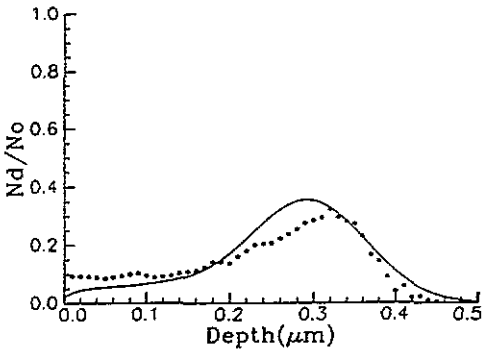

Figure 1. Damage profiles, represented by $N_d(x)/N_0$, of H^+-implanted ●, experimental data; ——, calculated data. X-cut: $LiNbO_3$ (50 keV; 3×10^{16} cm^{-2}) N_d is the displaced Nb atom concentration and N_0 is the total concentration.

element. The number of Nb atoms displaced from their normal crystal lattice sites [7] in $LiNbO_3$ is taken as a measurement of the total amount of the radiation damage; so the depth distribution of the displaced Nb atoms was determined by an iterative procedure based on a more reasonable plural-scattering theory [8]. We measured the damage profiles and these are represented by $N_d(x)/N_0$, where N_d and N_0 are the displaced Nb atom and the total Nb atom concentrations of H^+-implanted $LiNbO_3$ respectively. This roughly reflects the depth distribution of H^+ ions. Figure 1 shows the damage profile induced by H^+ implantation at room temperature.

When hydrogen was introduced into $LiNbO_3$, an infrared absorption band at about 3480 cm^{-1} was caused by the stretching vibration of the OH^- dipoles. The location of H^+ in the lattice is not definitely known, although the polarization dependence indicates that the OH^- dipoles lie on the oxygen plane. In Mg-doped $LiNbO_3$, the OH stretching vibration frequency increases from 3480 to 3535 cm^{-1} when the Mg doping level reaches a threshold concentration as reported by Bryan *et al* [9]. The new OH band has some component of absorption parallel to the *c* axis, which suggests that the OH dipoles are now slightly inclined with respect to the oxygen plane. Recently, in $LiNbO_3$ doubly doped with Mg and M (M≡Cr, Fe), in which the Mg doping level is above the threshold, a new absorption band has been found at about 3506 cm^{-1} in addition to the 3535 cm^{-1} peak [10, 11]. It was assumed to be caused by M^{3+}–OH^-–Mg^{2+} complex or the M^{3+} substitute for Nb^{5+} in the heavily Mg-doped $LiNbO_3$.

In the present study, the peak wavenumbers of the OH absorption spectra which were recorded using unpolarized light propagating perpendicular to the *c* axis are listed in table 2. The data on the OH band positions are in accordance with earlier observations reported by many researchers. The OH band in sample 2 which was obtained from a Li-rich melt exhibits a pronounced fine structure.

As shown in table 2, a new OH band at about 3545 cm^{-1} shows up in the H^+-implanted $LiNbO_3$. Furthermore, it was found that the new OH band is a rather broad unresolved band and its peak positions for all crystals listed in table 1 are nearly identical. The peak position seems to be independent of the stoichiometry, dopant species and doping levels in the samples investigated in the present study. The band is distinct from the well known band at 3480 cm^{-1} in undoped $LiNbO_3$ or in $LiNbO_3$ crystals with a lower Mg doping level. In the heavily Mg-doped $LiNbO_3$ this band partly overlaps the OH band at 3535 cm^{-1}. The width at half-maximum of the new OH band for sample 3 (5 mol% MgO), for sample 4 (6 mol% MgO) and sample 2 (Li rich) are 25 cm^{-1}, 18 cm^{-1} and 19 cm^{-1}, respectively. Figure 2 shows a H^+-implantation-induced OH band in a

Table 2. OH band positions in various $LiNbO_3$ crystals used in the present study.

Sample	Crystals	OH band positions (cm^{-1})
1	Congruent $LiNbO_3$	3480
2	Li-rich $LiNbO_3$	3462, 3482, 3488
3	Doped with 5 mol% MgO $LiNbO_3$	3480
4	Doped with 6 mol% MgO $LiNbO_3$	3535
5	Mg^+, Fe-doped $LiNbO_3$	3535, 3504
6	Cr-doped $LiNbO_3$	3480
7	Proton-implanted $LiNbO_3$	3545

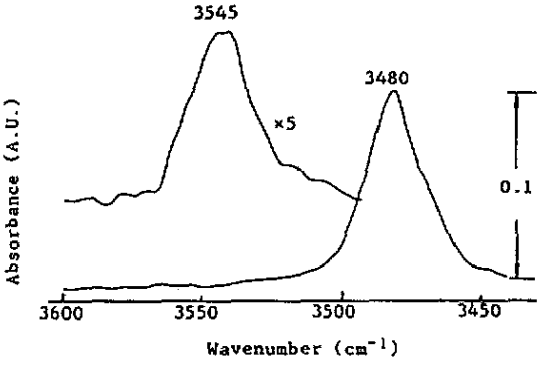

Figure 2. OH bands in a $LiNbO_3$ crystal: lower curve, as-grown $LiNbO_3$ from a congruent melt containing 5 mol% MgO (the thickness of the sample is 1 mm) upper curve, differential absorption spectrum of H^+-implanted $LiNbO_3$ with perfect $LiNbO_3$ as a reference.

$LiNbO_3$: Mg crystal (5 mol% MgO in congruent melt), in which the Mg doping level is below the threshold concentration according to our calculation and experiments [12]. It is noted that the stretching vibration energy of the OH band in the H^+-implanted $LiNbO_3$ seems to have the highest value known up to now for all $LiNbO_3$ crystals, including undoped, doped, heavily Mg-doped, Mg–M-codoped $LiNbO_3$ and proton-exchanged $LiNbO_3$. However, it is similar to the OH band in the neutron-irradiated $LiNbO_3$ reported by Gonzalez *et al* [13]. Both OH bands might result from an identical mechanism for radiation-induced hydrogen defects in $LiNbO_3$.

The infrared spectra of the H^+-implanted $LiNbO_3$ were also measured for the electric field vector both perpendicular and parallel to the *c* axis. The band intensity at 3545 cm^{-1} parallel to the *c* axis almost tends to vanish as in undoped $LiNbO_3$ or in $LiNbO_3$ with a lower Mg doping level. The result indicates that the OH dipoles in the H^+-implanted $LiNbO_3$ still lie in the oxygen plane perpendicular to the *c* axis.

The intensity of the OH band at 3545 cm^{-1} in H^+-implanted $LiNbO_3$ decreases slowly with time when the sample is in air at room temperature. After the sample had been annealed in air at 500 °C for 0.5 h, the band at 3545 cm^{-1} disappears.

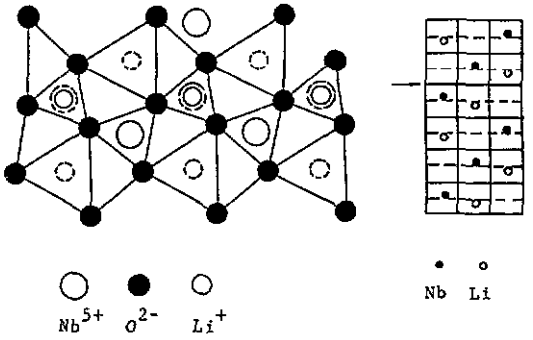

Figure 3. Schematic representation demonstrating the disposition of lattice ions on the oxygen plane (shown as arrow) viewed parallel to the *c* axis in a stoichiometric $LiNbO_3$ crystal. Circles drawn with full lines represent cations on the nearest lattice plane above the oxygen plane. Circles drawn with broken lines represent cations on the nearest lattice plane *below the oxygen plane.*

4. *Discussion*

The application, results and advantages of ion implantation for semiconductor production and integrated optics have been well documented for many years. Also, ion beams can also be used as diagnostic tools in the production and analysis of defect structure in insulating materials. In some cases, the ion-implantation-induced changes in optical absorption spectra can be used to study the mechanism of defect formation [14, 15].

In $LiNbO_3$, the hydrogen ion has a rapid diffusion rate and drift rate in an applied electric field. This is the result of the small size of proton. Therefore protons would tend to accumulate near the negatively charged centres under equilibrium conditions. Because $LiNbO_3$ is a typical non-stoichiometric compound, when the impurities are incorporated or crystal composition is changed, various charged centres attain another equilibrium state and result in corresponding OH bands. The situation is quite different in the case of H^+ implantation. Implanted hydrogen is uniformly distributed within the implanted region of the surface layer of $LiNbO_3$. Usually the defect concentration in $LiNbO_3$, including impurity ions and point defects caused by the non-stoichiometry such as (Nb_{Li}–V_{Nb}) complex defects [16], is less than 10%. Therefore most implanted protons would be in the undisturbed lattice region which is different from the lattice region disturbed by impurity ions or non-stoichiometric defects. In that case, implanted protons are as in a normal stoichiometric $LiNbO_3$ crystal, as shown in figure 3. During the ion implantation process, the damage is characterized by point defects mainly caused by the shift of Nb^{5+} ions from their regular sites to natural vacant octahedral sites on the *c* axis [17]. Thus the displacement of Nb^{5+} ions along the *c* axis can result in the movement of a higher positive charge away from one oxygen triangular plane of the octahedral site. This might be expected to decrease the interaction between Nb^{5+} ions and the oxygen triangular plane. Consequently, the displacement of Nb^{5+} ions may expand the oxygen triangle to result in longer O–O distances as shown in figure 4. The OH stretching vibrations in $LiNbO_3$ crystals can be interpreted by means of a local diatomic anharmonic oscillator [18]. Usually the longer O–O bond results in higher stretching frequency wavenumber of the OH absorption band in $LiNbO_3$ [19]. In addition an ion-implantation-induced volume expansion has been observed in ion-implanted $LiNbO_3$ [20]. The volume expansion is the same for *X*-cut and *Y*-cut $LiNbO_3$ but *Z*-cut $LiNbO_3$ exhibits a considerably smaller expansion. It also appears that the volume expansion effect would lead to a longer O–O distance.

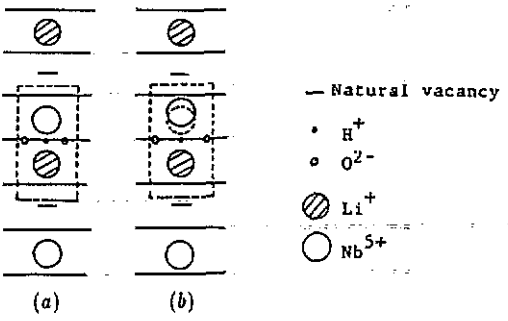

Figure 4. Schematic representation of the stoichiometric $LiNbO_3$ structure. The horizontal lines represent close-packed oxygen planes. The proton sits in the oxygen plane. The natural-vacancy sites are shown as — in the stacking sequence. (*b*) The lattice environment of the OH dipole in the H^+-implanted $LiNbO_3$ is compared with (*a*) the corresponding situation for the unimplanted $LiNbO_3$ lattice.

The intensity of the OH bond at 3545 cm^{-1} in H^+-implanted $LiNbO_3$ decreased with time. One can assume that the protons in the near-surface diffuse into the bulk of the crystal. When the sample was annealed in air at 500 °C, the damage in the lattice induced by H^+ implantation would be removed and the displaced Nb atoms would return to the normal lattice sites from the metastable positions.

Acknowledgment

This work was supported by the National Natural Science Foundation of China.

References

[1] Destefanis G L, Gailliard J P, Ligeon E L, Valette S, Farmery B W, Townsend P D and Perez A 1979 *J. Appl. Phys.* **50** 7898
[2] Wilson R G, Betts D A, Sadana D K, Zavada J M and Hunsperger R G 1976 *J. Appl. Phys.* **57** 5006
[3] Chandler P J and Townsend P D 1987 *Nucl. Instrum. Methods* **13** 921
[4] Shang Wei, Jiang Xin-yuan and Feng Xi-qi 1989 *Vacuum* **39** 287
[5] Feng Xi-qi and Shang Wei 1989 *Chinese Phys. Lett.* **6** 72
[6] Patrick L and Choyke W J 1973 *Phys. Rev.* B **8** 1660
[7] Feldman L C and Mayer J W 1986 *Fundamentals of Surface and Thin Film Analysis* (Amsterdam: North Holland)
[8] Meyer L 1971 *Phys. Status Solildi* b **44** 253
[9] Bryan D A, Rice R R, Gerson R, Tomaschke H E, Sweeney K L and Halliburton L E 1986 *Opt. Eng.* **24** 143
[10] Kovacs L, Foldvari I, Cravero I, Polgar K and Capelletti R 1988 *Phys. Lett.* **133A** 433
[11] Feng Xi-qi and Yin Ji-feng 1988 *Kexue Tongbao* **33** 851 (in Chinese)
[12] Feng Xi-qi, Zhang Qi-ren, Yin Ji-feng and Yin Zhi-wen 1990 *Sci. China, Ser.* A **33** 108
[13] Gonzalez R, Ballesteros C, Chen Y and Abrahan M M 1988 *Proc. Int. Conf. on Defects in Insulating Crystals (University of Parma 1988)* p 579
[14] Townsend P D 1981 *Nucl. Instrum. Methods* **182–3** 727
[15] Mattern P L, Thomas G J and Baller W 1976 *J. Vac. Sci. Technol.* **13** 430
[16] Krefft G B 1977 *J. Vac. Sci. Technol.* **14** 573
[17] Smyth D M 1986 *Proc. 6th Int. Symp. on Applications of Ferroelectrics (Leihigh University, June 1986)* IEEE Catalogue No. 86 CH2358-0 p 115
[18] Forster A, Kapphan S and Wholecke M 1987 *Phys. Status Solidi* b **143** 755
[19] Novak A 1974 *Struct. Bonding (Berlin)* **18** 177
[20] Destefanis G L, Townsend P D and Gailliard J P 1978 *Appl. Phys. Lett.* **32** 293